Thermal Performance Optimization of an Atrium as a Passive Solar System in a School Building

Mohammad Hossein Jahangir[1,*], and Fateme Rasaei[1]

[1] *Department of Renewable Energy Technologies and Energy Resources Engineering, University of Tehran, Tehran, Iran.*
**Corresponding author: mh.jahangir@ut.ac.ir*

Manuscript received 07 September, 2025; revised 17 August, 2026; accepted 18 September, 2026. Paper no. JEMT-2509-1572.

The increase in the global population, along with the industrialization of human life, has led to a daily rise in energy consumption. This trend has, in turn, contributed to issues such as greenhouse gas emissions. A significant portion of energy consumption is attributable to the building sector. Nowadays, various technologies, such as atriums, are employed to reduce energy consumption in buildings. In this study, four atrium designs were proposed and evaluated for a school building in Tehran. The Design Builder software was used to assess the respective systems. The results indicate that Sketches 3 and 4 are not energy-efficient and lead to an increase in the building's overall thermal load. In Sketch 2, the heating load decreased by 23.15%, while the cooling load increased by 9.59%, resulting in an overall reduction of the building's total thermal load by 7.56%. With Sketch 1, the heating load dropped by 19.52%, while the cooling load rise by 17.69%, leading to an overall decrease in the building's thermal load by 1.81%. Given that using an atrium increases the window-to-wall ratio, a concurrent reduction in heating load and increase in cooling load is expected. Based on the building's total thermal load, Sketch 2 is ultimately recommended as the optimal atrium design for this building. Implementing an atrium according to Sketch 2 would lead to a 7.56% reduction in the building's total thermal load.

Keywords: *Atrium, Passive Solar System, Energy Consumption, CO2 emission, Heating Load.*

http://dx.doi.org/10.22109/jemt.2026.545772.1572

Nomenclature

U_i	Mean air velocity in the x_i direction	$m.s^{-1}$
x_i	Direction of movement in the Cartesian coordinate system	m
x_j	Spatial coordinate in the j-direction (Cartesian coordinate system)	m
ρ	Air density	$kg.m^{-3}$
ϑ	Kinematic viscosity of air	$m^2.s^{-1}$
P	Air pressure	Pa
T	Air temperature	K
T_0	Reference temperature	K
g_i	Gravitational force in the x_i direction	
S_i	External forces	
μ_t	Turbulent dynamic viscosity of air	$kg.m^{-1}.s^{-1}$
k	Turbulent kinetic energy	
α	Thermal diffusivity	$m^2.s^{-1}$
c_p	Specific heat capacity	$J.kg^{-1}.K^{-1}$
S_e	Heat source term	
$q_{r,j}$	Radiative heat flux	
α_t	Turbulent thermal diffusivity	$m^2.s^{-1}$
G	Incident radiation	
n	Refractive index of the medium	$W.m^{-2}$
σ	Stefan-Boltzmann constant	$W.m^{-2}.K^{-4}$

1. Introduction

Greenhouse gas emissions in Iran, as a developing country, have been on the rise. The building sector consumes over 40% of the total energy produced in Iran, contributing approximately 25% of the nation's greenhouse gas emissions an amount of considerable significance [1]. Globally, this figure is around 46%, nearly double that of Iran, underscoring the worldwide nature of this concern [2]. Scientists, institutions, and policymakers in various countries are striving to reduce energy consumption or enhance energy system efficiency due to using new architectural and engineering solutions [3, 4]. The use of renewable energy sources [5], the adoption of advanced technologies to improve efficiency, and the development of systems known as zero-energy buildings have been introduced as key solutions in this area [6, 7]. Atrium systems, introduced as an emerging and evolving technology for optimizing cooling and heating systems to enhance energy efficiency, have been in use since the 19th century [8]. An atrium can essentially be defined as a designated space with specific dimensions and characteristics intended for energy transfer [9]. The advantages of utilizing these systems include reducing building heat loss through the roof and walls, enhancing natural ventilation by directing warm and cool air flows in the green roof, managing energy resources, and using renewable sources [10]. Tehran has a four-season climate, with somewhat warm summers and cold winters. Temperature variations across seasons contribute to increased heating and cooling loads in the city. Additionally, the high population of Tehran continually generates significant energy demands for both

cooling and heating.

Today, the use of atrium technology is growing and advancing toward maturity. This technology is employed in both cold and warm environments to reduce heating and cooling loads. Numerous studies have investigated the application of atrium technology for optimizing energy consumption or thermal load in buildings and evaluating the atrium effect [11]. Previous research findings have identified the key factors influencing atrium system efficiency, including atrium geometry, solar orientation, light penetration into adjacent spaces, light reflection from the atrium surface, light transmittance through the atrium, and geographic latitude [12-14]. Aizlewood et al.'s study was one of the earliest to examine atriums, presenting several methods for analyzing key radiative factors. It highlighted the significant impact of an atrium's location on energy efficiency [15]. Moosavi et al. identified the atrium's spatial position and form as the most influential parameters in its effectiveness for daylighting and ventilation [16]. Ahmad's study concluded that horizontally structured atriums with high lighting levels are unsuitable for hot climates [17]. In their study, Ghasemi et al. examined the performance of vertically oriented atriums with top lighting in Malaysia's hot climate and identified the optimal atrium model. Their findings showed that atriums with height-to-width ratios of 1:1, 1:3, and 1:3.8 performed best when adequate light was provided [14].

Further studies have explored the efficiency of atrium spaces for managing daily radiation and energy efficiency. Mohsenin and Hu analyzed the impact of daily radiation in atrium-equipped buildings using climate-based daylight modeling. Their study aimed to optimize atrium type selection and design ratios by incorporating variables such as atrium type, proportion, and ceiling diaphragm design. The results indicated that the well index was an effective measure for assessing ratios in climate-based modeling. The study also evaluated design parameters including climate, building thickness, material reflectance and transmittance, furniture, and monitor roof glass height, focusing on configurations where the monitor roof height equaled one-third or one-sixth of the wall height [18]. Aldawoud and Clark conducted a comparative study on the energy efficiency of courtyards and atriums, using central atriums and courtyards with identical specifications for comparison. Their results showed that open courtyard buildings demonstrated superior energy performance in low-rise structures. However, as building height increased, enclosed atriums often exhibited better energy efficiency. The optimal system at different heights depended on factors such as glazing and local climatic parameters [19]. The study by Moosavi et al. examined the performance and efficiency of atriums in a low-energy office building in tropical regions. They found that atrium-based systems, relying heavily on natural ventilation, are highly sensitive to solar radiation and incoming heat, which can compromise thermal comfort. To mitigate this issue, various design sketches were proposed for a building in Malaysia. The results revealed that an atrium featuring full cross-ventilation through all lobby entry openings, semi-accumulated chimney outlets, and a water wall with a high inlet-to-outlet surface area ratio achieved the best performance [20]. In the research by Chow et al., the atrium space was studied as a tool for controlling solar light in large areas. They emphasized that effective light management in circulation spaces, such as corridors, and ensuring adequate illumination, particularly in commercial and office environments, can significantly reduce electricity consumption. By regulating daily radiation, they evaluated the daylighting performance and energy efficiency of an atrium-based space, demonstrating that their proposed system captured 93% of daily radiation across four corridors [21]. Galal's study investigated the effect of materials above the atrium on daylight distribution and heat gain in a coastal region of Lebanon. The research began by analyzing the geographical and radiative characteristics of the area and used computer simulations to assess the impact of atrium design and material selection on these objectives. Various materials, including SGHC, DST, U-Factor, and VT, were evaluated. The findings indicated that, due to high annual solar radiation, prioritizing heat gain indicators over lighting performance is crucial in material selection [22].

Another category of research on atriums pertains to structural optimization. Aldawoud's study examined how atrium structure impacts building energy efficiency. Based on findings from various structural configurations, the research identified the optimal atrium design in terms of energy efficiency, ultimately recommending a layout featuring four central atriums. The analyzed atriums shared identical usage, area, structure, and control parameters. The results indicated that elongated atriums exhibited the lowest energy efficiency among the tested configurations [9]. Berardi and Wang examined the effect of angled atrium walls on natural ventilation and thermal performance in their study. Using computational fluid dynamics, they demonstrated that sloped walls enhance thermal comfort on lower floors by neutralizing pressure but reduce comfort on upper floors under neutral pressure. No significant advantage was found in using divergent walls compared to other layouts. They concluded that combining angled walls for lower floors with vertical walls for upper floors yields the best performance [23]. Ge et al. investigated how unenclosed atriums affect the thermal environment around shopping centers. Through field experiments, they analyzed heat source intensity, air infiltration rates, and temperature distribution in a multi-atrium center. The findings revealed that transmitted solar radiation and heat conduction through the atrium's glass roof significantly contributed to thermal stratification within internal spaces. Recognizing the impact of unenclosed atriums on the surrounding thermal environment, they recommended mitigating heat intensity by optimizing atrium form, glass roof design, and air infiltration adjustments [24]. Laouadi et al. studied the application of atrium technology in buildings to optimize thermal and energy efficiency. Using software simulations, they designed skylight elements while considering independent parameters such as sunlight and the atrium's physical characteristics. This method allowed for precise predictions of building temperatures, ensuring the energy consumption targets were met with the inclusion of the atrium. Additionally, other research has highlighted atriums as a key feature in energy-efficient architecture [25]. Rastegari et al. evaluated the use of atriums as an energy loss control strategy by analyzing an office building with an atrium in Tehran. They simultaneously assessed the well index and reflectance distribution index, and their findings revealed that a uniform reflectance model, striped patterns, and specific geometries significantly influence vertical daylight output [26]. Asfour studied atrium systems with varying window-to-wall ratios in Saudi Arabia's hot and arid climate. He recommended minimizing window areas and incorporating shaded daylight elements, such as courtyards and atriums, in these environments. Contrary to the common advice for minimal window use, his findings indicated that a 30% window-to-wall ratio provided balanced daylight performance, whereas ratios of 40% or higher increased cooling loads and caused visual discomfort due to glare [27]. In another study, Berardi and Wang investigated daylight performance in high-efficiency atrium buildings, focusing on glare using metrics such as instantaneous and cumulative radiation. Their findings emphasized that managing daily radiation is a significant challenge for atrium-based systems [23]. Beyraghshamshir and Sarkardehei analyzed heating and cooling efficiency in a school in Yazd using Design Builder simulations. Their study revealed that while atrium use positively impacted heating energy consumption, it also increased cooling loads, ultimately enhancing overall energy efficiency [28]. Xu et al. described the atrium as a complex thermal environment characterized by unique formation mechanisms. Their experimental analysis and statistical examination of parameters showed that precise atrium assessment can optimize ventilation and

heating systems, reduce energy consumption, and enhance thermal comfort [29]. Ratajczak et al. examined atrium spaces from both aesthetic and energy efficiency perspectives, simulating buildings where atriums functioned as independent and passive heating elements within HVAC systems. They analyzed two lighting control systems—timed on/off and daylight-dependent controls—and found that incorporating atriums into HVAC systems could reduce primary air heating energy by 17-22%. Additionally, adaptive lighting controls minimized instances of excessive heat, while atrium integration provided thermal comfort for over 90% of the useful time [30]. Jin et al. reported that HVAC systems account for over one-third of energy consumption in large buildings. Their study focused on a naturally ventilated public library in China, optimizing floor layout, building orientation, and interior structures to enhance natural ventilation through atrium spaces. They analyzed courtyards in two buildings, A and B, finding that thermal comfort was achieved in Building B but not in Building A due to excessive solar radiation. The proposed optimized system demonstrated a 46.54% energy savings while maintaining thermal comfort [31]. Pang et al. investigated the impact of atrium structural characteristics on energy efficiency in a hotel located in a cold region using computational fluid dynamics. The key structural features analyzed included atrium height, shape, and skylight area. Their results indicated that, with a fixed height, a smaller STH reduced energy consumption, while a larger WA at a constant height further decreased energy use [32]. Xiao et al. conducted a multi-objective optimization study of an atrium-based building in a Chinese city experiencing extreme seasonal temperatures. By optimizing building orientation, facade design, and interior space layout, they found that these adjustments could improve the energy use intensity (EUI) by 18.67% [33].

This study aims to optimize energy consumption management in a school in Tehran, with a focus on evaluating the use of atrium technology to achieve this goal. Initially, building plans will be prepared and sketch using geometric design software. Subsequently, using Design Builder software, the building's heating and cooling loads will be calculated and reported. The atrium system will then be incorporated into the simulation to manage the building's cooling and heating loads, evaluating various sketches. Using the results obtained, the impact of the atrium system on optimizing energy management in the target system will be explained. It is expected that implementing atrium systems will improve the thermal and cooling loads of the school, enhance energy resource management, and reduce heat losses through the school's roof and walls.

2. Methodology

Tehran, the capital of Iran, experiences hot summers and cold winters. The city is home to over 4,000 schools, serving approximately 1.18 million students. Due to Tehran's seasonal temperature fluctuations, both heating and cooling loads are substantial. This study investigates the impact of using an atrium on thermal performance, reducing energy load, and achieving thermal comfort in a school in Tehran. Initially, data on the climatic conditions of Tehran Province were gathered and reported from relevant sources. Subsequently, the school building was modeled in five configurations: the base model without an atrium and four alternative atrium configurations. The simulation and data analysis for this school were conducted using Design Builder software.

2.1. Building Specifications

The school building is located in Tehran and consists of eight classrooms four on the ground floor and four on the first floor. A workshop is located on the first floor, while the administration office is on the ground floor (Fig. 1). The two floors are connected by a staircase situated centrally on the building's northern side. Additionally, the school has a multipurpose hall at the entrance. Each classroom is equipped with two windows. The southern facade of the building features walls with angled windows and an atrium. Fig. 2 shows the northern view of the building, respectively.

Table 1. Building material specifications adopted for the studied school based on Iranian educational-building and national material guidelines [34-36].

Type of Space	Floor	Wall	Ceiling
Entrance Hallway	Ceramic tile, size 40x40 or 30x30	Stone block or paint finish	Suspended ceiling with insulation
Meeting and Communication Spaces	Ceramic tile, size 40x40 or 30x30	Stone block or paint finish	Suspended ceiling with insulation
Internal Corridors	Ceramic tile, size 40x40 or 30x30	Stone block or paint finish	Suspended ceiling with insulation
Classrooms, Multimedia and Science Labs	Ceramic tile, size 40x40 or 30x30	Stone block or paint finish	Suspended ceiling with insulation
Library/Reading Room	Stone, granite or travertine, size 30x30	Stone block, decorative paint	Plaster, painted white
Teachers' Room/Administration Office	Stone, granite or travertine, size 30x30	Stone block, decorative paint	Plaster, painted white
Auditorium	Stone, granite or travertine, size 30x30	Stone block, decorative paint	Plaster, painted white
Toilet and Washroom	Antislip ceramic tile, size 30x30	Tile up to 80cm, paint above	Suspended ceiling, water-resistant paint
Multipurpose Hall	Stone, granite or travertine, size 30x30	Stone block or paint finish	Plaster, painted white
Vocational Workshop	Stone, granite or travertine, size 30x30	Stone block or paint finish	Plaster, painted white
Storage Room	Stone, granite or travertine, size 30x30	Stone block or paint finish	Plaster, painted white
Garage	Concrete, rough finish	Stone block or paint finish	Concrete
Science Lab/Classroom	Stone or ceramic, size 30x30	Stone block or paint finish	Plaster, water-resistant paint
Terrace	Ceramic, waterproof coating	Waterproofed cement	Waterproof, white plaster
Greenhouse	Ceramic or stone, anti-slip finish	Stone block or paint finish	Transparent or translucent polycarbonate

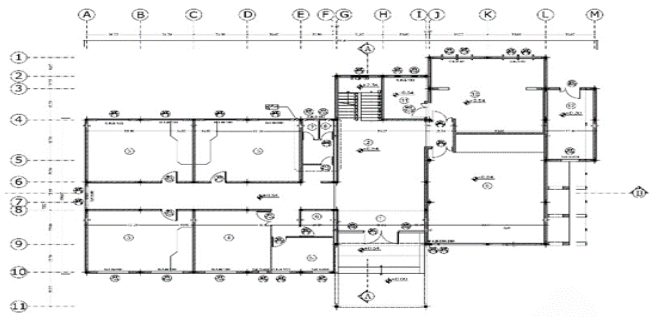

Fig. 1. Ground-Floor Architectural Plan of the Studied School Building

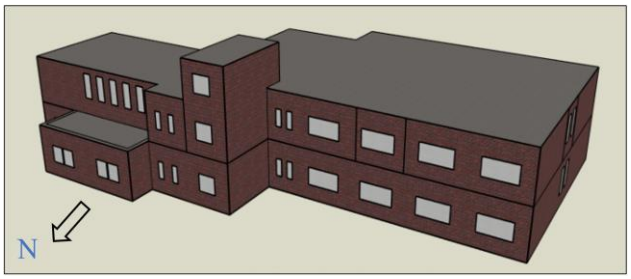

Fig. 2. North view of building.

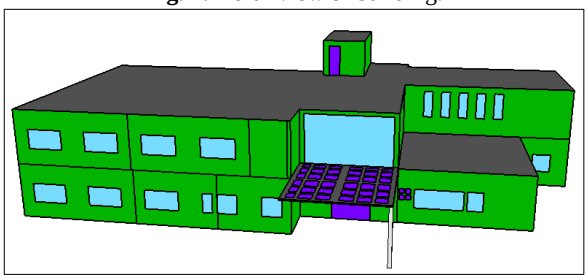

Fig. 3. Atrium Placement Above the Entrance Door (Sketch 1)

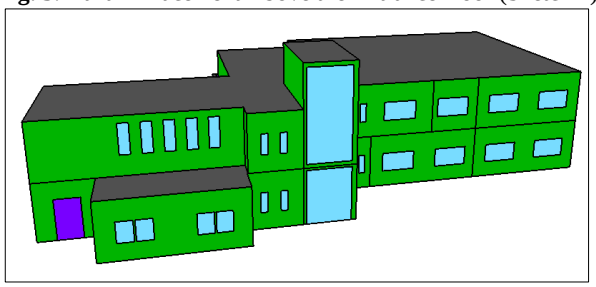

Fig. 4. Atrium Placement on the Northern Stairwell Wall (Sketch 2)

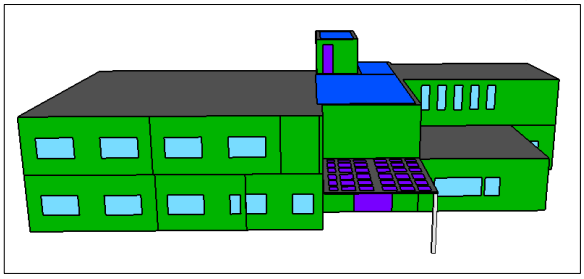

Fig. 5. Atrium Placement in the Central Portion of the First-Floor Ceiling (Sketch 3)

The school's location was set to Tehran using the Location tool in the software. The materials used in the construction of the building for each wall, floor, roof, and skirting board are listed in Table 1.

2.2. Atrium

Based on the building elevations shown in Fig. 2, the atrium can be considered in various configurations and orientations for different sides of the building. This study considers four distinct atrium sketches:

- The wall above the main entrance is considered as the atrium (Sketch 1).
- The staircase wall on the northern facade is considered as the atrium (Sketch 2).
- Only the central portion of the first-floor ceiling is considered as the atrium (Sketch 3).
- A combination of the wall above the main entrance, the staircase wall on the northern side, and the central portion of the first-floor ceiling are collectively considered as the atrium (Sketch 4).

The schematic layouts of Sketches 1–3 are shown in Figs. 3-5; Sketch 4 represents a combination of these three atrium locations.

These three sketches were selected because each chosen wall is part of the public corridor space, allowing any potential energy stored within the building to be transferred to other areas, if possible. All four sketches were analyzed, and the results were compared in terms of heating load, cooling load, lighting load, and thermal comfort. Finally, based on the obtained results, the optimal atrium placement design for the system was selected.

2.3. Mathematical modeling

To accurately determine airflow in CFD, it is essential to correctly set initial and boundary conditions, as well as select appropriate equations to describe flow turbulence. Various references suggest three models for turbulence analysis:

- Reynolds-Averaged Navier-Stokes (RANS) equations
- Large Eddy Simulation (LES)
- Direct Numerical Simulation (DNS) [37].

Airflow in natural ventilation systems involves fluid flow driven by buoyancy forces. The Boussinesq approximation is used to represent buoyancy force [38], assuming minimal temperature differences between indoor and outdoor air. Based on this assumption, continuity equations and Reynolds-Averaged Navier-Stokes equations in all three directions can be used for hourly simulations (Eq. 1-4) [39].

$$\nabla(\rho.u) + \frac{\partial \rho}{\partial t} = 0 \quad (1)$$

$$U_j \frac{\partial U_i}{\partial x_j} = -\frac{1}{\rho}\frac{\partial P}{\partial x_i} + \vartheta \frac{\partial^2 U_i}{\partial x_j \partial x_i} + \frac{1}{\rho}\frac{\partial\left(-\rho\,\overline{u_i' u_j'}\right)}{x_j} + S_i \quad (2)$$

$$U_j \frac{\partial U_i}{\partial y_j} = -\frac{1}{\rho}\frac{\partial P}{\partial y_i} + \vartheta \frac{\partial^2 U_i}{\partial y_j \partial y_i} + \frac{1}{\rho}\frac{\partial\left(-\rho\,\overline{u_i' u_j'}\right)}{y_j} + S_i \quad (3)$$

$$U_j \frac{\partial U_i}{\partial z_j} = -\frac{1}{\rho}\frac{\partial P}{\partial z_i} + \vartheta \frac{\partial^2 U_i}{\partial z_j \partial z_i} + \frac{1}{\rho}\frac{\partial\left(-\rho\,\overline{u_i' u_j'}\right)}{z_j} + g_i \frac{T_{T_0}}{T_0} + S_i \quad (4)$$

In the mentioned equations, U_i represents the mean air velocity in the x_i direction, measured in meters per second ($m.s^{-1}$). The variable x_i denotes the direction of movement in the Cartesian coordinate system, expressed in meters (m). ρ refers to the air density, measured in kilograms per cubic meter ($kg.m^{-3}$), while ϑ represents the kinematic viscosity of air, measured in square meters per second ($m^2.s^{-1}$). Additionally, P corresponds to the air pressure, expressed in Pascals (Pa). T is the air temperature, and T_0 indicates the reference temperature, both measured in Kelvin (K). The term g_i denotes the gravitational force in the x_i direction, and $S_i$accounts for external forces. The term $-\rho\,\overline{u_i' u_j'}$ represents the Reynolds stress, which is estimated using Eq. 5.

$$-\rho\,\overline{u_i' u_j'} = \mu_t\left(\frac{\partial U_i}{\partial x_j} + \frac{\partial U_j}{\partial x_i}\right) - \frac{2}{3}\rho k \delta_{ij} \quad (5)$$

In these equations, μ_t represents the turbulent dynamic viscosity of air, measured in $kg.m^{-1}.s^{-1}$, and k denotes the turbulent kinetic energy. The $k-epsilon$ turbulence model can be used to determine k [40]. Additionally, for each time step, heat transfer equations need to be solved. Generally, excluding heat transfer due to mass transfer, the overall heat transfer equation is defined as follows (Eq. 6) [38].

$$U_i \frac{\partial T}{\partial x_j} = \alpha \frac{\partial^2 T}{\partial x_j \partial x_j} + \frac{\partial\left(\overline{-T' u_j'}\right)}{\partial x_j} - \frac{1}{\rho c_p}\frac{\partial q_{r,j}}{\partial x_j} + S_e \quad (6)$$

This equation defines α as the thermal diffusivity, measured in square meters per second ($m^2.s^{-1}$). The term c_p represents the specific heat capacity, expressed in joules per kilogram per kelvin($J.kg^{-1}.K^{-1}$).Additionally, $S_e$denotes the heat source term, and $q_{r,j}$describes the radiative heat flux. The term $-T'u_j'$ represents the

fluctuation term, which can be approximated using Eq. 7.

$$\overline{-T'u_j'} = \alpha_t \frac{\partial T}{\partial x_j} \quad (7)$$

In this equation, α_t represents the turbulent thermal diffusivity, measured in $m^2.s^{-1}$. Additionally, Eq. 8 is used to calculate q_r [41].

$$-\frac{\partial q_{r,j}}{\partial x_j} = \alpha G - 4\alpha n^2 \sigma T^4 \quad (8)$$

In this equation $q_{r,j}$ represents the radiative heat flux in the j-direction ($W.m^{-2}$), and x_j is the spatial coordinate in the j-direction (m). α is the thermal diffusivity ($m^2.s^{-1}$), while G denotes the incident radiation ($W.m^{-2}$). n is the refractive index (dimensionless), σ is the Stefan-Boltzmann constant (5.67×10^{-8} $W.m^{-2}.K^{-4}$), and T is the absolute temperature (K). These parameters are used to analyze radiative heat transfer and thermal properties. With the recent equations and by applying appropriate boundary and initial conditions to the defined geometry, the velocity and temperature distributions can be calculated.

3. Results

The simulation of the system was conducted using Design Builder V7.2.6 with the Energy Plus 9.4 computational engine. Calculations related to CFD, cooling and heating loads, and thermal comfort temperatures were performed. The analysis of each criterion for the four sketches is discussed in the following sections. Initially, the base model needs to be simulated to assess system behavior under various cooling and heating conditions. The simulation results indicate that the building has substantial heating and cooling loads, as expected. The building has an area of 9,822.12 ft², requiring an annual heating load of 69,984.35 kBtu and a cooling load of 242,995.39 kBtu. This corresponds to an area-specific cooling intensity of 24.74 kBtu/ft² and a heating intensity of 7.13 kBtu/ft². The building's heating load is 267.210 kBtu/h, and the cooling load is 242.78 kBtu/h. In educational buildings, cooling and heating for thermal comfort are among the primary energy consumers. According to standards, the thermal comfort range is between 20-25°C. In summer, cooling systems like air conditioners are used to prevent excessive temperature rise, and in winter, heating systems like radiators maintain minimum temperatures. The energy consumption for these loads is significant, and associated costs are considerable. Therefore, it is essential to evaluate the designed systems from various perspectives. In the following, Figs. 6-10 sequentially present the results obtained from the simulation of the intended system during the school's operational months. These Figures illustrate temperature, relative humidity, heating load, cooling load, and carbon dioxide emissions.

According to Fig. 6, across all sketches, the temperature remains relatively stable throughout the year, without any significant increases or decreases. This suggests that the heating and cooling systems have largely managed to maintain the temperature within a specified range. According to human comfort standards, the ideal temperature for schools should be between 20-25 °C. It is observed that the temperature in most months and under all sketches is approximately within this range, indicating the effective performance of heating and cooling systems. However, in warmer months (such as June), some sketches reach higher temperatures, which may require further adjustments. As second criteria for human comfort Fig. 7 shows the relative humidity.

For comfort, relative humidity should be within the 30-60% range. For thermal comfort, a relative humidity range of 30–60% is generally considered acceptable. As shown in Fig. 7, the relative humidity values remain relatively stable across the different atrium configurations; however, in several operational months, the values fall below the lower limit of 30%. Therefore, although the atrium configurations have only a limited influence on indoor relative humidity, additional humidity control may be required during the drier periods to maintain desirable indoor environmental conditions. To achieve stable condition in a building, heating and cooling system are essential. Fig. 8 and Fig**. 9** demonstrate the heating and cooling system duty.

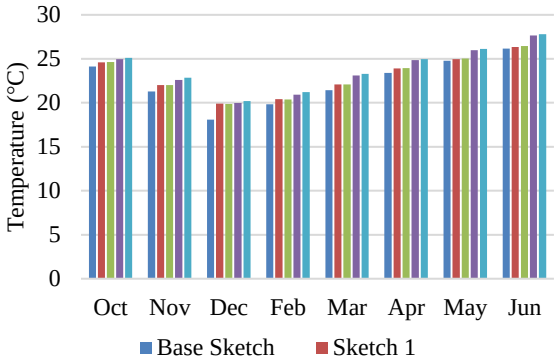

Fig. 6. Indoor temperature of the school during operational months

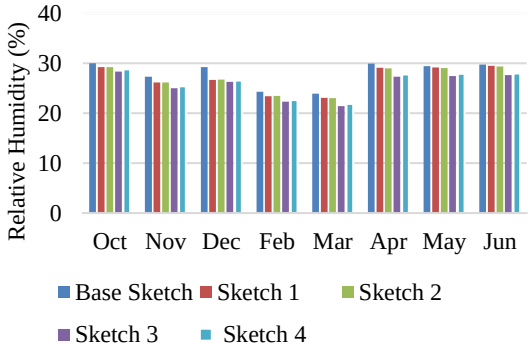

Fig. 7. Air relative humidity of school during operational months

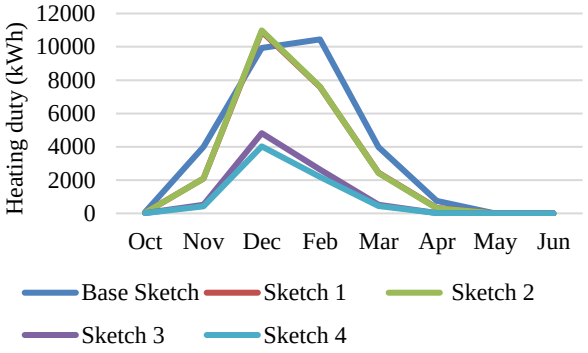

Fig. 8. Heating duty during operational months

In Fig. 8, which shows the heating duty, a notable increase in heating requirements is observed during the colder months (November to February) across all sketches. This indicates a higher demand for heating to maintain a comfortable indoor temperature during winter. Among the sketches, "Base Sketch" and "Sketch 2" exhibit the highest heating loads in December and January, while "Sketch 3" and "Sketch 4" require comparatively less heating. This suggests that "Sketch 3" and "Sketch 4" may be more energy-efficient and optimized for heating purposes. As the weather warms up from March onwards, the heating demand declines significantly, reaching nearly zero in all sketches, reflecting the reduced need for heating.

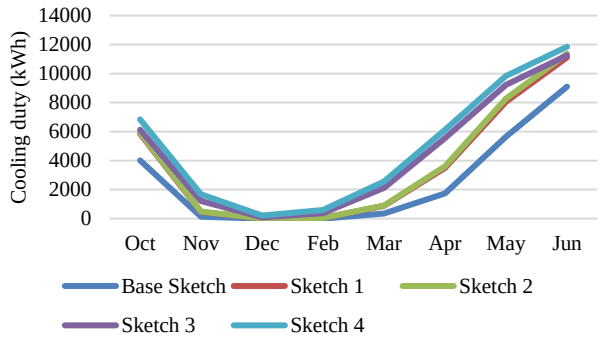

Fig. 9. Cooling duty during operational months

In Fig. 9, which depicts the cooling duty, there is an opposite trend, with an increase in cooling requirements during the warmer months, particularly from April onward. This increase reflects the need for cooling to maintain comfort in the school environment as temperatures rise. During the hottest months, especially in June, "Sketch 2" and "Sketch 4" show the highest cooling demands, while "Base Sketch" and "Sketch 1" require relatively less cooling. These differences are mainly associated with the changes in atrium configuration, glazing area, solar exposure, and the resulting heat gains in each sketch. Variations in the atrium geometry can alter solar heat gain and heat transfer through the building envelope, thereby affecting the cooling demand during warmer months. In the intermediate months, the cooling load across all sketches is relatively similar, indicating comparable performance of the cooling systems during these periods. In summary, the different sketches have varying impacts on the energy required for heating and cooling. Overall, the atrium configurations affect heating and cooling demands differently throughout the year. Although some configurations may show relatively low heating requirements during particular months, the annual comparison presented in Table 2 indicates that Sketch 2 provides the greatest overall reduction in heating load. At the same time, all atrium configurations increase the cooling load relative to the Base Sketch, with Sketch 2 showing the smallest increase. Another valuable result for comparing different Sketches is the analysis of carbon dioxide emission graphs. Fig. 10 presents the carbon dioxide emission for considered Sketches.

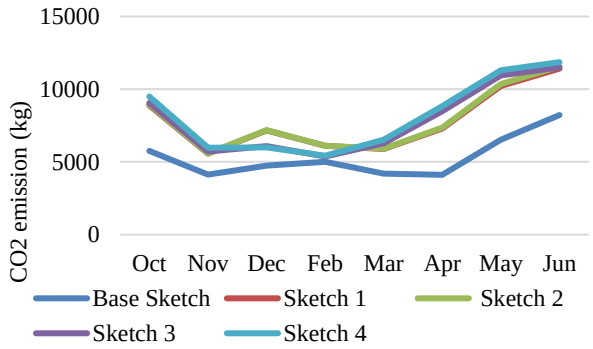

Fig. 10. CO_2 emission during operational month

According to results shown in Fig. 10, the carbon dioxide emissions in the Base Sketch are consistently lower compared to other Sketches, indicating its more efficient performance. In this Sketch, the lowest emissions are observed in November and December, followed by a gradual increase from February onwards, eventually reaching its peak in June, though it remains lower than the other Sketches throughout. Sketches 1, 2, 3, and 4 exhibit a nearly similar trend. Their emissions decrease in the early months and, after a period of relative stability, show a clear upward trend starting from March. By June, these Sketches reach almost similar emission levels, reflecting a comparable design or operational pattern among them. Sketches 1 and 2, on average, have demonstrated lower carbon dioxide emissions compared to Sketches 3 and 4. This suggests that the design or operational parameters of Sketches 1 and 2 may be relatively more effective in reducing emissions, despite following a similar overall trend in emission levels across the months.

The results indicate that, for all four Sketches considered, the indoor temperature is well-controlled and remains close to the comfort temperature range. To compare the performance of these four sketches and select the best option for implementation, it is necessary to extract the data presented in the charts numerically and compare them with each other.

Table **1** provides comparative calculations of the cooling and heating loads for each of the four sketches, along with the Base Sketch.

Table 1. The cooling and heating load results for different Sketches (negative values indicate a decrease, and positive values indicate an increase)

Sketch Name	Cooling Load (kBtu/h)	Heating Load (kBtu/h)	Percentage Change Compared to Base (Cooling Load)	Percentage Change Compared to Base (Heating Load)
Base Sketch	242.78	267.21	-	-
Sketch 1	285.73	215.04	+17.69%	-19.52%
Sketch 2	266.07	205.35	+9.59%	-23.15%
Sketch 3	387.99	227.03	+59.81%	-15.03%
Sketch 4	397.27	230.93	+63.63%	-13.57%

The obtained data indicate that incorporating an atrium in this building has generally led to an increase in cooling load and a decrease in heating load. The greatest reduction in heating load is observed in Sketch 2, while the smallest reduction in heating load is found in Sketch 4. Considering heating load reduction as a comparison criterion, the order of suitability for the sketches is Sketch 2, Sketch 1, Sketch 3, and Sketch 4. On the other hand, the highest increase in cooling load is associated with Sketch 4, and the smallest increase in cooling load is related to Sketch 2. Using cooling load increase as a comparison criterion, the suitable sketches in order are Sketch 2, Sketch 1, Sketch 3, and Sketch 4. Additionally, the total cooling and heating loads for each sketch should also be compared with the Base Sketch to determine whether the overall thermal load of the building increases or decreases with each sketch. Table 2 presents the total cooling and heating load data for the building, along with the percentage of reduction or increase compared to the Base Sketch.

Table 2. The total thermal load data for different Sketches (negative values indicate a decrease, and positive values indicate an increase)

Sketch Name	Total Thermal Load (kBtu/h)	Percentage Change Compared to Base Sketch
Base Sketch	509.99	-
Sketch 1	500.77	-1.81%
Sketch 2	471.42	-7.56%
Sketch 3	615.02	+20.59%
Sketch 4	628.20	+23.17%

The results presented in Table 2 indicate that Sketch 2 has the highest reduction, while Sketch 4 shows the highest increase in the building's total thermal load. Sketches 3 and 4 lead to an increase in the building's thermal load, making them unfavorable from an energy consumption perspective. Therefore, Sketches 1 and 2 are considered energy-saving options. For further analysis of the results, the annual

daylighting for the Base Sketch and Sketch 2 have been compared. This comparison aims to provide deeper insights into the performance differences between these two Sketches, particularly in terms of their daylighting efficiency and its potential impact on overall energy consumption and carbon dioxide emissions. Fig. 11 and Fig**. 12** are annual daylighting for Base Sketch and Sketch 2.

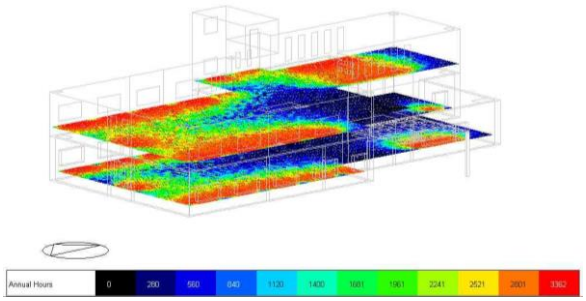

Fig. 11. Annual daylighting for Base Sketch

Fig. 11 shows the Annual Daylighting distribution for the Base Sketch. Areas near windows receive ample natural light (yellow to red), while interior zones rely heavily on artificial lighting (blue to green). This uneven distribution suggests higher energy use and carbon emissions for interior lighting. Improving daylight penetration through skylights or window adjustments could enhance energy efficiency. Comparing these results with Sketch 2 will provide further insights into design impacts on energy performance.

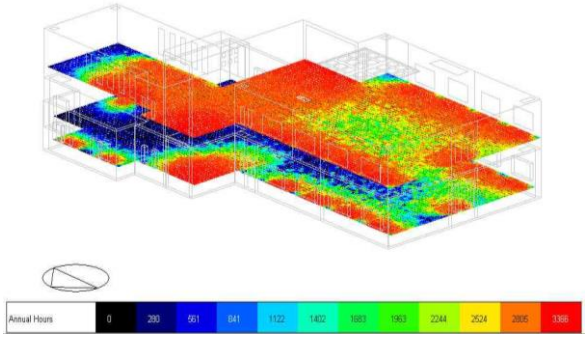

Fig. 12. Annual daylighting for Sketch 2

Fig. 12 shows the Annual Daylighting distribution for Sketch 2, which can be compared with Fig. 11 (Base Sketch). In Sketch 2, daylighting appears significantly improved in interior zones, with more areas showing higher exposure (yellow to red hues). Compared to the Base Sketch, Sketch 2 achieves better light penetration into central spaces, reducing reliance on artificial lighting. While the Base Sketch had limited daylighting in interior regions (blue to green), Sketch 2 demonstrates a more uniform distribution, especially in open areas. This suggests that design modifications in Sketch 2, such as increased openings or reflective surfaces, enhance daylighting efficiency. Compared with the Base Sketch, Sketch 2 demonstrates a more uniform daylight distribution and improved light penetration into the interior zones. This improvement may reduce the dependence on artificial lighting during occupied hours. However, the overall effect on total energy consumption and CO_2 emissions should be evaluated together with the heating and cooling demands, since the CO_2 emission results presented in Fig. 10 do not indicate a reduction relative to the Base Sketch.

4. Conclusions

Sketches 1 and 2 have improved the building's thermal performance. The results indicate that Sketches 3 and 4 are not justified in terms of energy consumption and are therefore deemed unsuitable. With Sketch 2, the heating load decreases by 23.15%, while the cooling load increases by 9.59%. Overall, the total thermal load of the building is reduced by 7.56%. In the case of Sketch 1, the building's heating load decreases by 19.52%, whereas the cooling load increases by 17.69%. Additionally, the total thermal load of the building decreases by 1.81%. The reduction in heating load can be attributed to the increased solar heat gain associated with the atrium glazing and the resulting changes in heat transfer through the building envelope. However, the same increase in solar exposure and glazing area can result in additional heat gains during warmer periods, thereby increasing the building's cooling load. Based on the results, Sketch 2 represents the most favorable atrium configuration because it provides the greatest reduction in heating load while causing the smallest increase in cooling load among the four atrium alternatives. From the perspective of carbon dioxide emissions, the Base Sketch has demonstrated lower emissions compared to the other Sketches. Among the four considered Sketches, Sketches 1 and 2 exhibited similar behavior and showed lower emissions compared to the other two Sketches. The annual daylighting analysis also showed that Sketch 2 provides improved daylight penetration and a more uniform daylight distribution compared with the Base Sketch. Overall, considering the combined heating and cooling loads, Sketch 2 was identified as the most favorable atrium configuration for the studied school building.

References

[1] O. Rahmani, S. Rezania, A. Beiranvand Pour, S. M. Aminpour, M. Soltani, Y. Ghaderpour, and B. Oryani, "An overview of household energy consumption and carbon dioxide emissions in Iran", Processes, vol. 8, 2020.

[2] W. F. Lamb, T. Wiedmann, J. Pongratz, R. Andrew, M. Crippa, J. G. J. Olivier, D. Wiedenhofer, G. Mattioli, A. Al Khourdajie, J. House, S. Pachauri, M. Figueroa, Y. Saheb, R. Slade, K. Hubacek, L. Sun, S. K. Ribeiro, S. Khennas, S. De La Rue Du Can, L. Chapungu, S. J. Davis, I. Bashmakov, H. Dai, S. Dhakal, X. Tan, Y. Geng, B. Gu, and J. Minx, "A review of trends and drivers of greenhouse gas emissions by sector from 1990 to 2018", Environmental Research Letters, vol. 16, 2021.

[3] C. I. Ezeh, Y. Hong, W. Deng, and H. Zhao, "High rise office building makeovers—Exploiting architectural and engineering factors in designing sustainable buildings in different climate zones", Energy Reports, vol. 8, pp. 6396-6410, 2022.

[4] F. Rasaei, H. Yousefi, M. Razeghi, A. Naseri, M. Abdoos, and R. Ghasempour, "Optimal selection of CSP site for desalination system using GIS and AHP method in Hormozgan province, Iran", Energy Reports, vol. 13, pp. 2255-2268, 2025.

[5] M. H. Jahangir and F. Rasaei, "Techno-economic and life cycle assessment of an energy harvesting system from urban traffic using piezoelectric plates: Case study on a highway", e-Prime – Nexus of Electrical, Electronic, and Intelligent Engineering, vol. 17, 2026.

[6] D. H. W. Li, L. Yang, and J. C. Lam, "Zero energy buildings and sustainable development implications – A review", Energy, vol. 54, pp. 1-10, 2013.

[7] L. Belussi, B. Barozzi, A. Bellazzi, L. Danza, A. Devitofrancesco, C. Fanciulli, M. Ghellere, G. Guazzi, I. Meroni, F. Salamone, F. Scamoni, and C. Scrosati, "A review of performance of zero energy buildings and energy efficiency solutions", Journal of Building Engineering, vol. 25, 2019.

[8] S. Sharples and D. Lash, "Daylight in atrium buildings: A critical review", Architectural Science Review, vol. 50, pp. 301-312, 2007.

[9] A. Aldawoud, "The influence of the atrium geometry on the building energy performance", Energy and Buildings, vol. 57, pp. 1-5, 2013.

[10] D. Utkucu and H. Sözer, "An evaluation process for natural ventilation using a scenario-based multi-criteria and multi-interaction analysis", Energy Reports, vol. 6, pp. 644-661, 2020.
[11] Y. Hong, C. I. Ezeh, W. Deng, J. Lu, Y. Ma, and Y. Jin, "Climate adaptation of design scheme for energy-conserving high-rise buildings-Comparative study of achieving building sustainability in different climate scenarios", Energy Reports, vol. 8, pp. 13735-13752, 2022.
[12] B. Calcagni and M. Paroncini, "Daylight factor prediction in atria building designs", Solar Energy, vol. 76, pp. 669-682, 2004.
[13] M. Ghasemi, M. Noroozi, M. Kazemzadeh, and M. Roshan, "The influence of well geometry on the daylight performance of atrium adjoining spaces: A parametric study", Journal of Building Engineering, vol. 3, pp. 39-47, 2015.
[14] M. Ghasemi, M. Z. Kandar, and M. Noroozi, "Investigating the effect of well geometry on the daylight performance in the adjoining spaces of vertical top-lit atrium buildings", Indoor and Built Environment, vol. 25, pp. 934-948, 2016.
[15] M. E. Aizlewood, "The daylighting of atria: A critical review", ASHRAE Transactions, vol. 101, pp. 841-857, 1995.
[16] L. Moosavi, N. Mahyuddin, N. Ab Ghafar, and M. A. Ismail, "Thermal performance of atria: An overview of natural ventilation effective designs", Renewable and Sustainable Energy Reviews, vol. 34, pp. 654-670, 2014.
[17] M. H. Ahmad, "The Influence of Roof Form and Interior Cross Section on Daylighting in the Atrium Spaces in Malaysia", Ph.D. thesis, University of Manchester, 1996.
[18] M. Mohsenin and J. Hu, "Assessing daylight performance in atrium buildings by using Climate Based Daylight Modeling", Solar Energy, vol. 119, pp. 553-560, 2015.
[19] A. Aldawoud and R. Clark, "Comparative analysis of energy performance between courtyard and atrium in buildings", Energy and Buildings, vol. 40, pp. 209-214, 2008.
[20] L. Moosavi, N. Mahyuddin, and N. Ghafar, "Atrium cooling performance in a low energy office building in the Tropics, a field study", Building and Environment, vol. 94, pp. 384-394, 2015.
[21] S. K. H. Chow, D. H. W. Li, E. W. M. Lee, and J. C. Lam, "Analysis and prediction of daylighting and energy performance in atrium spaces using daylight-linked lighting controls", Applied Energy, vol. 112, pp. 1016-1024, 2013.
[22] K. S. Galal, "The impact of atrium top materials on daylight distribution and heat gain in the Lebanese coastal zone", Alexandria Engineering Journal, vol. 58, pp. 659-676, 2019.
[23] U. Berardi and T. Wang, "Daylighting in an atrium-type high performance house", Building and Environment, vol. 76, pp. 92-104, 2014.
[24] J. Ge, Y. Zhao, and K. Zhao, "Impact of a non-enclosed atrium on the surrounding thermal environment in shopping malls", Journal of Building Engineering, vol. 35, 2021.
[25] A. Laouadi, M. Atif, and A. Galasiu, "Methodology towards developing skylight design tools for thermal and energy performance of atriums in cold climates", Building and Environment, vol. 38, pp. 117-127, 2003.
[26] M. Rastegari, S. Pournaseri, and H. Sanaieian, "Analysis of daylight metrics based on the daylight autonomy (DLA) and lux illuminance in a real office building atrium in Tehran", Energy, vol. 263, 2023.
[27] O. S. Asfour, "A comparison between the daylighting and energy performance of courtyard and atrium buildings considering the hot climate of Saudi Arabia", Journal of Building Engineering, vol. 30, 2020.
[28] M. Beyraghshamshir and E. Sarkardehei, "A comparison of the cooling and heating performance of two passive systems of central courtyards and atriums at an elementary school in Yazd City", Solar Energy, vol. 252, pp. 156-162, 2023.
[29] C. Xu, Y. Wang, J. Hui, L. Wang, W. Yao, and L. Sun, "Study on winter thermal environmental characteristics of the atrium space of teaching building in China's cold region", Journal of Building Engineering, vol. 67, 2023.
[30] K. Ratajczak, K. Bandurski, and A. Płóciennik, "Incorporating an atrium as a HAVC element for energy consumption reduction and thermal comfort improvement in a Polish climate", Energy and Buildings, vol. 277, 2022.
[31] Z. Jin, Y. Zhang, H. Sun, M. Han, Y. Zheng, Y. Zhao, W. Han, and M. Zhang, "Indoor thermal nonuniformity of atrium-centered public building: Monitoring and diagnosis for energy saving", Case Studies in Thermal Engineering, vol. 54, 2024.
[32] J. Pang, Z. Fan, M. Yang, J. Liu, R. Zhang, W. Wang, and L. Sun, "Effects of complex spatial atrium geometric parameters on the energy performance of hotels in a cold climate zone in China", Journal of Building Engineering, vol. 72, 2023.
[33] W. Xiao, W. Zhong, H. Wu, and T. Zhang, "Multiobjective optimization of daylighting, energy, and thermal performance for form variables in atrium buildings in China's hot summer and cold winter climate", Energy and Buildings, vol. 297, 2023.
[34] M. Ansary, "A comparative study of design standards of educational spaces in primary schools of Iran and Finland", Iranian Journal of Comparative Education, vol. 8, pp. 3878-3904, 2025.
[35] Plan and Budget Organization of the Country, "Design Criteria for Educational Buildings (Standardized Architectural Programming for Primary and Middle Schools)," Center for Documents, Records, and Publications, 2017.
[36] M. Talaei and H. Sangin, "Multi-objective optimization of energy and daylight performance for school envelopes in desert, semi-arid, and mediterranean climates of Iran", Building and Environment, vol. 255, 2024.
[37] J. L. M. Hensen and R. Lamberts, Eds., "Building Performance Simulation for Design and Operation", Spon Press, 2011.
[38] R. B. Bird, "Transport phenomena", Applied Mechanics Reviews, vol. 55, 2002.
[39] S.-H. Peng, "Modelling of Turbulent Flow and Heat Transfer for Building Ventilation", Ph.D. thesis, Chalmers University of Technology, 1998.
[40] B. E. Launder and D. B. Spalding, "The numerical computation of turbulent flows in Numerical Prediction of Flow, Heat Transfer, Turbulence and Combustion", Pergamon Press, pp. 96-116, 1983.
[41] J. R. Mahan, "Radiation Heat Transfer: A Statistical Approach", John Wiley & Sons, 2002.